UK Heat Transfer Conference 2021
UKHTC2021

17th UK Heat Transfer Conference (UKHTC2021)
4-6 April 2022, Manchester, UK

NUMERICAL SIMULATION ON FLOW BOILING HEAT TRANSFER OF PCM-R134A SLURRY IN A MICROCHANNEL

Ren Yang*, Yi Wang, Yulong Ding, Yongliang Li

Birmingham Centre for Energy Storage, School of Chemical Engineering, University of Birmingham, Edgbaston, Birmingham B15 2TT, United Kingdom

1. ABSTRACT

In present work, numerical investigations were conducted on flow boiling heat transfer of R134a with phase change material (PCM) particles in a 2D horizontal microchannel (0.5 mm width × 20 mm length). The VOF model with LEE model was used for the simulation and the effect of PCM melting on the overall heat transfer was addressed with an effective PCM heat capacity method. The mass transfer intensive factor r_i in Lee model was deliberately selected and validated with the experimental data of R134a flow boiling at saturated temperature of 31℃ in a microchannel. Then, the effects of inlet concentration and latent heat of PCM on the multiphase heat transfer performance, including the overall heat transfer coefficient (HTC) and pressure drop, were evaluated at mass fluxes of 200 and 400 $kg/m^2 \cdot s^{-1}$ and a constant heat flux of 69 kW/m^2. Results indicate that by introducing PCM melting to the base fluid, the overall flow boiling HTC was enhanced significantly while the vapor fractions of R134a on heating surfaces and in bulk fluid were both decreased. Furthermore, with the addition of PCM particles, the pressure drop of R134a flowing through the microchannel was increased when the latent heats of PCM were small but decreased at large latent heats as the inlet PCM concentration increased. It was also found that flow pattern transition in microchannel was delayed from elongated slug flow to nucleating/bubbly flow when comparing the situations with and without PCM particles at the same boundary conditions, which may be attributed to the higher thermal conductivity of PCM and extra endothermic heat associated with PCM melting in base fluid. Therefore, multiphase flow of R134a/PCM slurries in microchannel might be a promising approach with superior heat dissipating capability for thermal management of high power density electronics.

2. INTRODUCTION

Flow boiling in microchannels has been employed for thermal management of electronic devices. However, there remains some challenging issues needed to be resolved for better practical applications such as high pressure drop, deterioration of cooling capability and flow instability at high heat fluxes [1]. To improve heat transfer performance in microchannels, one approach is to add some functional additives to working fluids such as encapsulated phase change material (EPCM) particles with high specific heat during phase change and nanoparticles with high thermal conductivity [2]. Recently, numerous experimental studies were conducted to investigate flow boiling of nanofluid. Some results are inconsistent and even contradictory in microchannels [3]. However, few relevant work has been conducted in published literature to investigate the PCM melting effect on flow boiling heat transfer in microchannels. In present work, numerical simulations were conducted to investigate flow boiling heat transfer of a pure coolant with PCM particles suspended in microchannel.

R134a is an alternative coolant for multiphase flow cooling in electronic device as it is a dielectric super–wetting fluid which could be evaporated within the temperature limits of electronic components. Marcinichen et al. [4] pointed out that the chip temperature of microprocessors should be kept below 85℃ to maintain high-level performance at reliable and sustainable conditions.

Numerical simulation is an effective alternative tool to understand complex heat transfer processes. Recently, there are some multiphase methods to simulate flow boiling heat transfer of pure fluids, such as the Eulerian-Eulerian/RPI wall boiling method (EE-RPI) [5] and the Volume of Fluid / Lee method

*Corresponding Author: rxy812@student.bham.ac.uk

(VOF-LEE) [6]. Generally, the EE-RPI method is more suitable for highly subcooled flow boiling in macrochannel, while the VOF-LEE method takes more account for bubble dynamics and flow patterns in micro/minichannel at large vapor quality cases. Additionally, there are two types of methods regard simulating convective heat transfer of fluids containing functional particles: single and two-phase methods [7]. While the liquid-particle mixture in single-phase method is assumed as a homogeneous fluid with only one group of average effective properties for the entire fluid, the liquid-particle mixture is treated as two separate phases, liquid and solid, with distinct group of properties for each phase in two-phase method. It was found that the VOF model is a proper option for simulating fluids with high particle concentrations and has decent accuracy towards experimental data under acceptable costs [8]. Therefore, the VOF-LEE coupled with an effective heat capacity method was used to investigate flow boiling of R134a-based latent heat functional fluids in a microchannel. The effects of melting latent heat, particle concentrations and mass fluxes on flow boiling heat transfer performance including HTC, pressure drop and Figure of Merit (FOM) were evaluated at a consistent heat flux conditions.

3. MATHEMATICAL MODEL AND VALIDATION

3.1 Physical and mathematical models

Flow boiling of functional fluid with suspended PCM particles melting in a microchannel is a very complex heat and mass transfer phenomenon. To balance the computing resources while maintaining acceptable numerical convergence and simulation accuracy, the present numerical simulation model was simplified under the following assumptions and special treatments: 1) Coolant is separated into three continuous phases: liquid R134a, vapor R134a and a suspended cloud of PCM particles. Particles are assumed to be mixed with liquid R134a in a stable and homogeneous state, which means that the particles movements are dominantly driven by evaporation occurred in the domain while the mutual forces (e.g. particles with particles, bubbles and walls etc.) are ignored. 2) R134a-based functional fluid is considered as a Newtonian-like and incompressible fluid, based on results in literature [9].

This work simulated multiphase flow of R134a-based functional fluid in a 2D horizontal domain (0.5mm width×20mm length×0.05mm thickness of stainless steel) at a constant heating flux condition. A non-uniform quadrilateral mesh, gradually refined towards the heating walls, was adopted to capture small-size bubbles in viscous boundary layers. Inlet temperature and PCM melting temperature were set as 30℃ and 30.5℃, respectively. Properties of R134a were chosen at the saturated temperature of 31℃. Contact angle and the surface tension of R134a were set as 2° and 7.3×10^{-3} n/m [10,11].

As mentioned before, there are three separate immiscible phases in flow boiling of functional fluid. The multiphase VOF method was used to track the interfaces between different phases in domain. The gravity effect was ignored in this study [12]. These major control equations are listed as follows.

$$\frac{\partial(\alpha_q\rho_q)}{\partial t}+\nabla\cdot(\alpha_q\rho_q\vec{v}_q)=S_{m,pq} \tag{1}$$

$$\sum_{q=1}^{3}\alpha_q=1 \tag{2}$$

$$\frac{\partial(\rho\vec{v})}{\partial t}+\nabla\cdot(\rho\vec{v}\vec{v})=-\nabla p+\nabla\cdot\left[\mu\left(\nabla\vec{v}+\nabla\vec{v}^T\right)\right]+\vec{F}_{surf} \tag{3}$$

$$\frac{\partial(\rho E)}{\partial t}+\nabla\cdot[\vec{v}(\rho E+p)]=\nabla\cdot\left(k_{eff}\nabla T\right)+S_h \tag{4}$$

$$\rho=\sum_{q=1}^{3}\alpha_q\rho_q \qquad E=\frac{\sum_{q=1}^{3}\alpha_q\rho_q E_q}{\sum_{q=1}^{3}\alpha_q\rho_q} \tag{5}$$

Where α_q, ρ_q and $\vec{v}_q$ are volume fraction, density and velocity of phase "q" in (1-2), respectively. While ρ, μ and k_{eff} are the volume-averaged values of density, dynamic viscosity and effective thermal conductivity, E and T are the mass-averaged values of energy and temperature in (3-5). Sum of three volume fractions is equal to unity. Surface tension force $\vec{F}_{surf}$ is considered as a source term calculated by continuum surface force method. $S_{m,pq}$ and S_h are the mass and energy source terms from phase "p" to phase "q" in phase change process. While the mass flux exchange between liquid and vapor R134a phases was calculated by LEE model, the values between suspended particle phase with liquid and/or vapor R134a phases were set to zero.

LEE model is a simplified Schrage model, considering quasi-thermo-equilibrium phase change at a constant pressure and driven by the deviation of local temperature from saturated temperature [43].

$$\begin{cases} S_{m,pq} = - S_{m,qp} = - r_i \alpha_q \rho_q \left| \frac{T - T_{sat}}{T_{sat}} \right|, T < T_{sat} \\ S_{m,pq} = - S_{m,qp} = + r_i \alpha_q \rho_q \left| \frac{T - T_{sat}}{T_{sat}} \right|, T > T_{sat} \end{cases} \tag{6}$$

$$S_h = S_{m,pq} \cdot q_{LH} \tag{7}$$

where, q_{LH} is latent heat of evaporation and r_i is an empirical relaxation factor with the unit of s^{-1}. The proper value of r_i should be determined by various factors such as the mesh size, the operational condition and channel configuration for specific cases[13]. In present work, the values were chosen by fitting simulation results with corresponding experimental data.

For the PCM solid-liquid melting process, an effective heat capacity method (rectangular stepped profile [14]) and an effective viscosity model (VAND [15]) were used to take into account its effect on flow boiling heat transfer in microchannel at EPCM concentration less than 25%vol.. The realizable k-ε model was adopted as the turbulent model. The PISO algorithm was chosen for the pressure-velocity coupling, as well as the second-order upwind for momentum and energy equations, the PRESTO and Geo-Reconstruct discretization for pressure and volume fraction interpolation. The absolute residual of continuity equation was set to $1e^{-4}$.

3.2 Mesh independence test and model validation

Mesh independence test was carried out based on R134a flow boiling in the microchannel at 200 kg/(m^2·s) and 16 kW/m^2. The area-averaged R134a vapor fraction on heating walls (i.e. x_{wall}) are used as the mesh independence indicator, which is plotted against flow time revolution and averaged grid size in Fig.1 (left). It was noticed that when the grid size was less than 10 µm, its variation with further mesh refinement was less than 3%. The grid size was fine enough to capture tiny bubbles generated on heating surfaces. Therefore, 10 µm grid size was selected for the simulations.

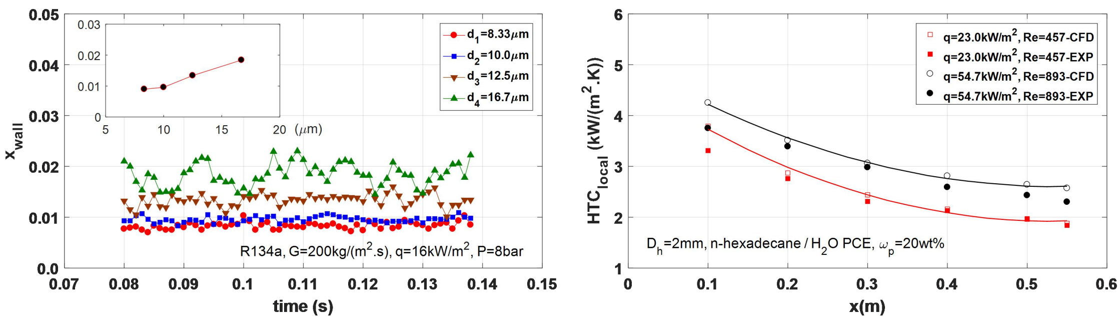

Figure 1: (left) Grid independent test based on the vapor fraction on heating walls of R134a. (right) Comparisons of local HTCs of n-hexadecane/H_2O emulsion (with PCM melting in liquid water) in a minichannel [16]

To ensure the satisfactory accuracy, an empirical factor "r_i" in Lee model was validated with some experimental data of R134a flow boiling in a ϕ1.1 mm tube [17,18,19]. According to the assessment of local HTCs at the exit and pressure drop shown in Fig.2, it was chosen as 2500 for 200 kg/(m^2·s) or 6500 for 400 kg/(m^2·s) at 69 kW/m^2, respectively. Importantly, the factor r_i is assumed to be the same for R134a-based functional fluid at the similar conditions. Furthermore, the effective PCM heat capacity method was also validated with experimental data of single phase convective heat transfer in a ϕ2mm tube by adding 20%wt. nanosize n-hexadecane melting in water shown in Fig.1 (right) [16].

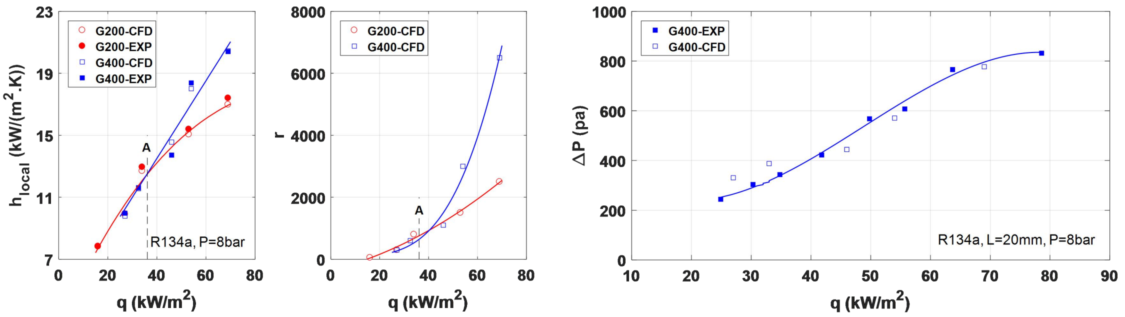

Figure 2: Comparisons of pure R134a flow boiling heat transfer between numerical and experimental cases (left) local HTCs [17,18] and (right) pressure drop in a micro/minichannel [19]

4. PRELIMINARY RESULTS

The effects of inlet concentration (~25 %vol.) and the latent heat per melting temperature (~417.4 kJ/kg·K^{-1}) of PCMs on multiphase flow heat transfer of PCM-R134a slurries at inlet temperature 30°C, mass fluxes of 200, 400 kg/(m^2·s) and heat flux 69 kW/m^2 were investigated and compared with pure R134a flow boiling in microchannel. It is worth noting that thermal conductivity of selected PCM (n-Octadecane) is 4.9 times that of liquid R134a and the evaporating latent heat of R134a is 173 kJ/kg.

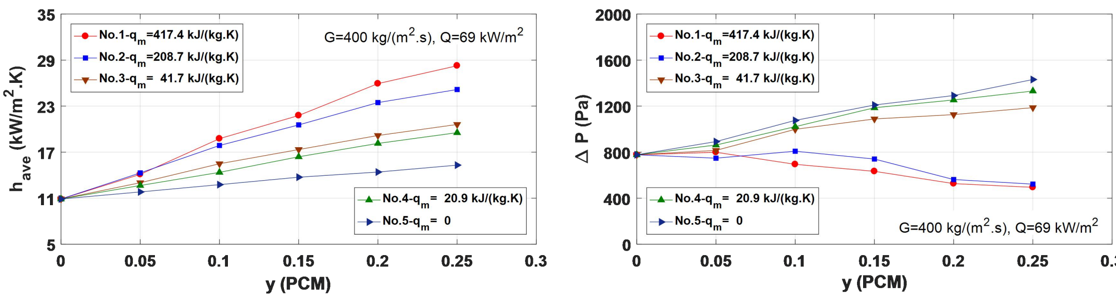

Figure 3: Effect of inlet concentration and latent heat rate of PCM on (left) the overall HTC and (right) pressure drop of R134a/PCM slurry in the microchannel. (The latent heat rate is defined as latent heat per melting temperature of PCM)

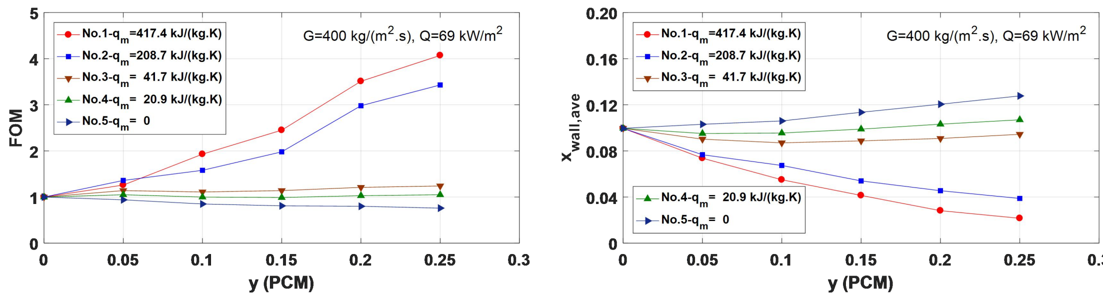

Figure 4: Effect of inlet concentration and latent heat rate of PCM on (left) FOM and (right) vapor fraction of R134a/PCM slurry on heating surfaces in a microchannel. (The latent heat rate is defined as latent heat per melting temperature of PCM)

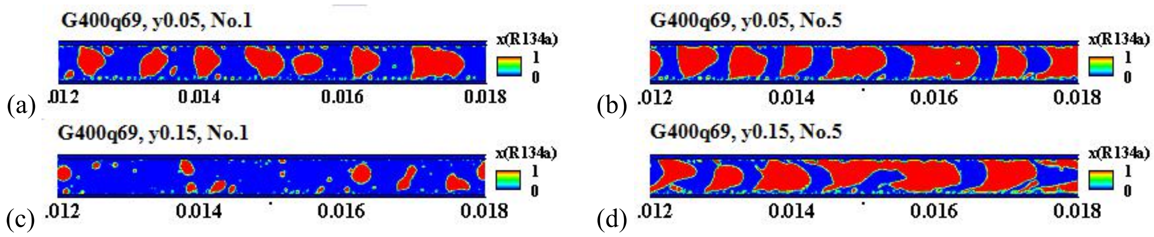

Figure 5: Vapor fraction distribution of R134a/EPCM multiphase flow under different inlet concentration and latent heat rate of PCM in a microchannel. (No.1 and No.5 indicate the cases with 417.4 and 0 kJ/(kg·K) respectively)

As shown in Fig.3 (left), the flow boiling HTCs of R134a/PCM slurry linearly increase with inlet concentrations for different latent heats and a greater latent heat rate of PCM leads to a larger HTC value at the same concentration. Latent heat rate is defined as latent heat per melting temperature of PCM. Taking the cases with concentration of 15%vol. as example, while the HTC was enhanced to 13.7 kW/(m^2·K) by adding nanoparticles with thermal conductivity 4.9 times that of liquid R134a for case No.5, it was increased to 17.3 and 20.5 kW/(m^2·K) by adding PCM particles with latent heat rate of 41.7 kJ/(kg·K) at case No.3 and 208.7 kJ/(kg·K) at case No.2, in comparison with 10.9 kW/(m^2·K) of pure R134a, respectively. On the other hand, according to Fig.3 (right), the average pressure drop increased with PCM concentrations when the latent heat rate was less than 41.7 kJ/(kg·K), but kept almost constant at small concentrations and decreased significantly in cases with concentration greater than 10%vol., when the latent heat rate was larger than 208.7 kJ/(kg·K). Correspondingly, comparing to R134a, the nanofluid (at No.5) could decrease figure of merit (FOM) in Fig.4 (left), but the PCM slurry could increase it even though its enhancement was tiny effected with the concentrations when latent heat rate of PCM was smaller than 41.7 kJ/(kg·K). For case of No.2 with latent heat rate of 208.7 kJ/(kg·K), the FOMs of 15%vol. and 25%vol. PCM slurry were twice and 3.4 times that of pure R134a, respectively.

Furthermore, while the vapor fraction of R134a on heating walls of nanofluid (at No.5) increased with inlet concentrations in Fig.4 (right), it decreased quickly with increased inlet concentration when the latent heat rate of PCM was larger than 208.7 kJ/(kg·K) such as No.1. The corresponding flow patterns are illustrated in Fig. 5, where the flow pattern transition for R134a/PCM slurry at No.1 was suppressed from large-size bubbly flow (a) to nucleating flow (c) due to increased PCM concentration and effective heat capacity, whereas the flow pattern turned into intermittent slug flow (d) for case No.5 without PCM melting when increasing the concentration from 5% to 15% vol..

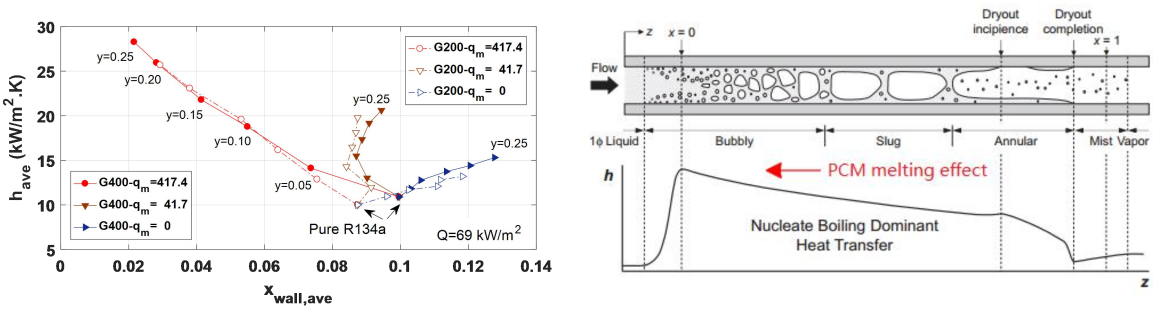

Figure 6: Relation (left) the overall HTC VS vapor fraction on heating surfaces and (right) schematics of flow regimes and local HTC in microchannels at a uniform heat flux condition adapted from [20].

According to the relations of HTC vs. vapor qualities at different mass fluxes and latent heat rates in Fig.6 (left), it is the endothermal melting effect related to latent heat rates and inlet concentrations, which could decrease vapor fractions on surfaces and inhibit flow pattern transition at a constant heat flux, that increases HTC and decreases pressure drop in the nucleating boiling dominant heat transfer (i.e. the red arrow in Fig.6 (right)).

5. CONCLUSIONS

Flow boiling of R134a/PCM slurries with PCM melting in microchannels is a promising approach to further enhance heat dissipating capacity in corresponding application. It is the endothermal melting effect related to latent heat and inlet concentration, which could reduce the vapor fractions on heating surfaces and then prevent adverse flow pattern transitions, that not only improves flow boiling HTC but also lowers pressure drop throughout the microchannel.

REFERENCES

[1] Y.K. Prajapati, P. Bhandari, Flow boiling instabilities in microchannels and their promising solutions – a review, Exp. Therm. Fluid Sci. 88 (2017) 576–593.

[2] T.G. Karayiannis, M.M. Mahmoud, Flow boiling in microchannels: Fundamentals and applications, Appl. Therm. Eng. 115 (2017) 1372–1397.

[3] B. Jacqueline, D. Brutin, and L. Tadrist. A review on boiling heat transfer enhancement with nanofluids. Nanoscale research letters 6.1 (2011) 1-16.

[4] J.B. Marcinichen, J.A. Olivier, N. Lamaison, J.R. Thome, Advances in electronics cooling, Heat Transfer Eng. 34(5-6) (2013) 434-446.

[5] M. Colombo, M. Fairweather, Accuracy of Eulerian-Eulerian, two-fluid CFD boiling models of subcooled boiling flows, Int. J. Heat Mass Transf. 103 (2016) 28-44.

[6] C.R. Kharangate, I. Mudawar, Review of computational studies on boiling and condensation, Int. J. Heat Mass Transfer 108 (2017) 1164-1196.

[7] M. Akbari, N. Galanis, A. Behzadmehr, Comparative analysis of single and two phase models for CFD studies of nanofluid heat transfer, Int. J. Therm. Sci. 50 (2011) 1343-1354.

[8] M.K. Moraveji, R.M. Ardehali, CFD modeling (comparing single and two-phase approaches) on thermal performance of Al2O3/water nano fluid in mini-channel heat sink, Int. Commun. Heat Mass Transf 44 (2013) 157–164.

[9] X. Wang, J. Niu, Y. Li, X. Wang, B. Chen, R. Zeng, Q. Song, Flow and heat transfer behaviors of phase change material slurries in a horizontal circular tube, Int. J. Heat Mass Transf. 50 (2007) 2480-2491.

[10] C.L. Ong, J.R. Thome, Flow boiling heat transfer of R134a, R236fa and R245fa in a horizontal 1.03 mm circular channel, Exp. Therm. Fluid Sci. 33 (2009) 651– 663.

[11] Lu. Xingbin, Jinping Liu, Xu. Xiongwen, Contact angle measurements of pure refrigerants, Int. J. Heat Mass Transfer 102 (2016) 877–883.

[12] R. Revellin, V. Dupont, T. Ursenbacher, J.R. Thome, I. Zun, Characterization of diabatic two-phase flows in microchannels: flow parameter results for R-134a in a 0.5 mm channel, Int. J. Multiphase Flow 32 (2006) 755–774.

[13] L. Yang, W. Li, J.Z. Zhang, W.J. Minkowycz. Analysis of thermal performance and pressure loss of subcooled flow boiling in manifold microchannel heat sink. Int. J. Heat Mass Transfer 162 (2020): 120362.

[14] L. Chai, R. Shaukat, L. Wang, H.S. Wang, A review on heat transfer and hydrodynamic characteristics of nano/microencapsulated phase change slurry (N/MPCS) in mini/microchannel heat sinks, Appl. Therm. Eng. 135 (2018) 334–349.

[15] H. Dai, W. Chen, Q. Cheng, Y. Liu, Analysis of thermo-hydraulic characteristics in the porous-wall microchannel with microencapsulated phase change slurry, Int. J. Heat Mass Transf. 165 (2021) 120634.

[16] F. Ma, J. Chen, P. Zhang, Experimental study of the hydraulic and thermal performances of nano-sized phase change emulsion in horizontal mini-tubes, Energy 149 (2018) 944–953.

[17] D. Shiferaw, T.G. Karayiannis, D.B.R. Kenning, Flow boiling in a 1.1 mm tube with R134a: experimental results and a comparison with model, Int. J. Therm. Sci. 48 (2009) 331–341.

[18] T.G. Karayiannis, D. Shiferaw, D.R. Kenning, V.V. Wadekar, Flow patterns and heat transfer for flow boiling in small to micro diameter tubes, Heat Transfer Eng. 31 (2010) 257–275.

[19] M.M. Mahmoud, T.G. Karayiannis, D.B.R. Kenning, Flow boiling pressure drop of R134a in microdiameter tubes: Experimental results and assessment of correlations, Heat Transf. Eng. 35 (2) (2014) 178–192.

[20] S.-M. Kim, I. Mudawar, Review of databases and predictive methods for heat transfer in condensing and boiling mini/micro-channel flows, Int. J. Heat Mass Transfer 77 (2014) 627–652.